Electron magneto-tunneling through single self-assembled InAs quantum dashes

2014 Appl. Phys. Express 7 045001

(http://iopscience.iop.org/1882-0786/7/4/045001)

Applied Physics Express 7, 045001 (2014)
http://dx.doi.org/10.7567/APEX.7.045001

Electron magneto-tunneling through single self-assembled InAs quantum dashes

Kenji Shibata[1*†], Nikola Pascher[2], Perttu J. J. Luukko[3], Esa Räsänen[3,4], Stephan Schnez[2], Thomas Ihn[2], Klaus Ensslin[2], and Kazuhiko Hirakawa[1,5]

[1]*INQIE and IIS, University of Tokyo, Meguro, Tokyo 153-8505, Japan*
[2]*Solid State Physics Laboratory, ETH Zürich, 8093 Zürich, Switzerland*
[3]*Nanoscience Center, Department of Physics, University of Jyväskylä, FI-40014 Jyväskylä, Finland*
[4]*Department of Physics, Tampere University of Technology, FI-33101 Tampere, Finland*
[5]*CREST-JST, Kawaguchi, Saitama 332-0012, Japan*
E-mail: kshibata@iis.u-tokyo.ac.jp

Received February 18, 2014; accepted March 10, 2014; published online March 28, 2014

We have investigated electron magneto-tunneling through single self-assembled InAs quantum dashes (QDHs) coupled to metal nanogap electrodes. The samples operate as single electron transistors and exhibit clear shell structures, reflecting the anisotropic shape of the QDHs. In high magnetic fields, the samples exhibit strongly orbital-dependent large diamagnetic shifts and large electron *g*-factors in the range $|g| \sim 3$–11. The strong level-to-level fluctuation of the *g*-factors implies the presence of strong spin–orbit interaction in this system. These properties suggest that InAs QDHs are promising for the manipulation of single-electron orbital/spin states by external electric/magnetic fields.

Control of the spin degrees of freedom in semiconductor quantum dots (QDs) has been widely studied for quantum information processing and spintronic applications.[1–5] Self-assembled InAs QDs have unique atomlike properties and exhibit electrically tunable large electron *g*-factors and strong spin–orbit interactions,[6–8] which are important for the electrical/magnetic manipulation and readout of single charge/spin states in QDs. Self-assembled InAs quantum dashes (QDHs) with highly anisotropic wirelike shapes grown on (211)B-oriented GaAs substrates are larger than ordinary self-assembled InAs QDs.[9,10] Large InAs nanostructures are known to be favorable for realizing electrically tunable large electron *g*-factors and strong spin–orbit interactions. QDHs are therefore good candidates for applications to spintronic and quantum information devices. In a previous paper, the basic transport characteristics of QDHs in the many- and few-electron regimes were discussed.[10] However, the electronic properties of QDHs in the magnetic field have not yet been characterized in detail.

In this work, we have investigated electron magneto-tunneling through single self-assembled InAs QDHs coupled to ferromagnetic (FM) Ni nanogap electrodes for their application to spintronic devices.[4,5] The fabricated QDH samples operate as single-electron transistors and exhibit clear shell structures, reflecting the anisotropic shape of InAs QDHs. Moreover, the samples exhibit orbital-dependent large diamagnetic shifts and large electron *g*-factors. By utilizing these properties of InAs QDHs, we may efficiently control single-electron orbital/spin states using external electric/magnetic fields.

Self-assembled InAs QDHs were grown by molecular beam epitaxy on (211)B-oriented n^+-GaAs substrates. After successively growing a 20-nm-thick $Al_{0.3}Ga_{0.7}As$ barrier layer and a 200-nm-thick undoped GaAs buffer layer, InAs QDHs were grown at 490 °C.[10] FM Ni metal source–drain electrodes with a nanogap (gap size: 30–50 nm) were formed directly on the QDHs by electron beam lithography. Prior to the metal deposition, the sample wafers were dipped into buffered hydrofluoric acid for 5 s to remove native oxides on the QDH surfaces. The n-type substrate was used as a backgate electrode to tune the electronic states in the InAs QDHs.[5,10]

Figure 1(a) shows a Coulomb stability diagram obtained by plotting the differential conductance dI/dV_{SD} as a function of the source–drain voltage V_{SD} and the backgate voltage V_G. As seen in Fig. 1(a), the conductance and size of the Coulomb diamonds strongly depend on the electron number N in the QDH, and the conductance gradually increases with increasing N [see also Fig. 2(a)]; these tendencies indicate that the electron wavefunction in the QDH becomes more extended in space with increasing N.[11] Figure 1(b) shows the addition energy as a function of N derived from Fig. 1(a). The role of the anisotropic shape in the electronic properties of InAs QDHs was studied previously,[10] where the measured addition energy spectrum of a QDH sample was reproduced with spin-density-functional calculations, taking into account the geometry of the device as observed by SEM imaging. Here, we carried out spin-density-functional calculations for the sample shown in Fig. 1. We found excellent agreement between the experimental and theoretical addition energies, as shown in Fig. 1(b).[12] The inset shows the optimized confining potential that is found to have a shape with almost linear confinement in the transverse direction and slightly steeper, roughly third-order polynomial walls in the longitudinal direction. This confining potential shape is very different from that in the previously analyzed QDH sample (parabolic wall in the transverse direction and fifth-order polynomial wall in the longitudinal direction).[10] In the previous report, we used the top-gate structure to tune the electronic states in the QDHs and access the few-electron regime, which makes the confining potential shape more complicated because of the screening of the top-gate electric field by metal nanogap electrodes. Therefore, this variation may arise from how we apply the gate electric fields. The lateral confinement size of electrons in the QDH was determined to be $\sim 110 \times 50\,nm^2$ in the calculation, which is considerably smaller than the metallurgical size of the QDH seen in the inset of Fig. 1(a). The difference suggests that in the few-N regime, the electrons are confined close to the center of the QDH. In addition, it is likely that a QDH longer than 300 nm may not be of a single domain and

†Present address: Department of Electronics and Intelligent Systems, Tohoku Institute of Technology, Sendai 982-8577, Japan.

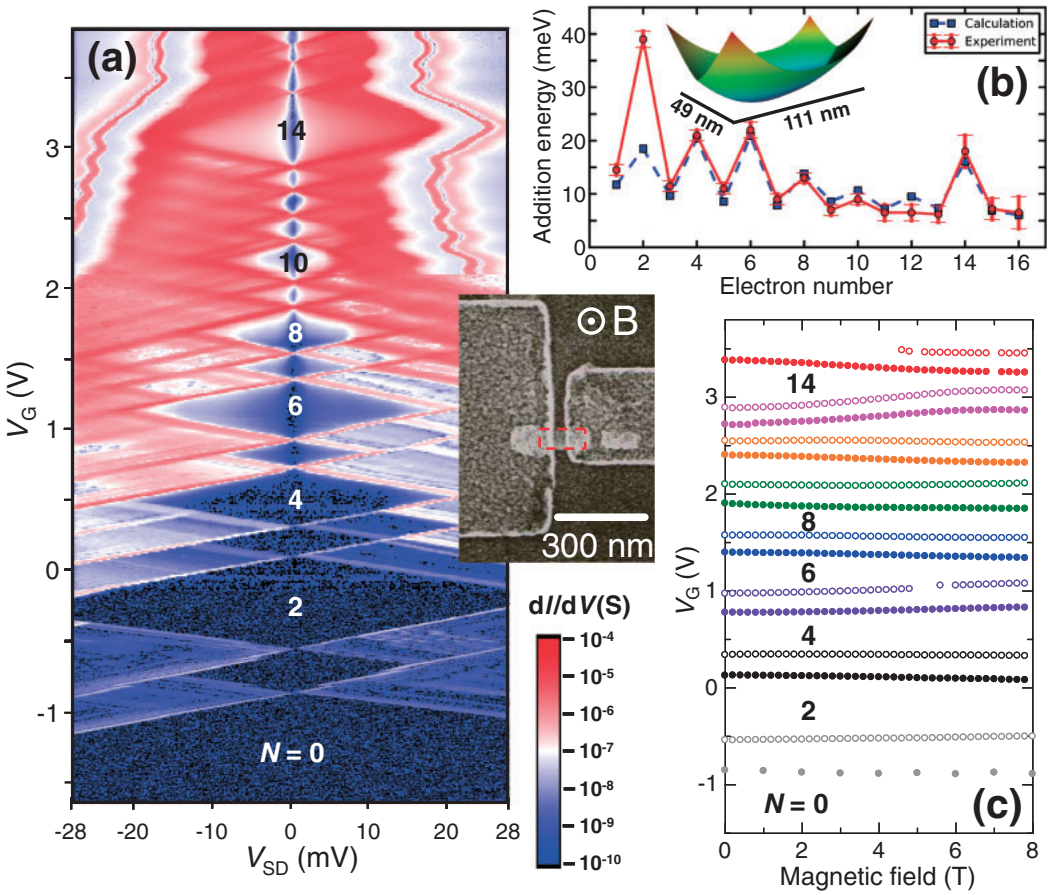

Fig. 1. (a) Coulomb stability diagram measured at electron temperature of ~250 mK in zero magnetic field. The number of electrons N in each Coulomb diamond is also shown. The inset shows an SEM image of the fabricated QDH sample. The red dashed line is a guide for the eye. (b) Addition energies experimentally determined as a function of N compared with the spin-density-functional calculations. (c) Magnetic field dependence of Coulomb oscillation peak positions. The magnetic field was applied perpendicular to the GaAs surface. Pairs of the Coulomb peaks displayed by open and closed circles in the same colors are well described by the same diamagnetic coefficients and therefore attributed to the doublet states.

we detect electron tunneling only through one of the domains in the region surrounded by the red dashed line in the inset of Fig. 1(a).

Figure 1(c) shows Coulomb peak positions as a function of magnetic field B perpendicular to the GaAs surface. It is found that two bunched Coulomb peaks (1st and 2nd, 3rd and 4th, etc.) exhibit almost the same conductance, as shown in Fig. 2(a), and are well described by the same diamagnetic shift [see also Fig. 2(b)]. Therefore, these paired peaks are attributed to the doublet states. Figure 2(b) shows the shift of the Coulomb peak positions with increasing B-field for the paired 3rd and 4th Coulomb peaks. Both curves are well described by the same diamagnetic coefficient $\gamma_{3\text{–}4} \sim -18$ $\mu eV/T^2$ [solid lines in Fig. 2(b)]. Figure 2(c) shows the B-field evolution of the gate voltage spacing δV_G for the paired 3rd and 4th Coulomb peaks. δV_G increases linearly with increasing B-field, indicating the lifting of the spin degeneracy owing to Zeeman splitting. From this behavior, the electron g-factor is determined to be $|g| \sim 4.5$ for these doublet states. Figure 2(d) shows the B-field dependence of the ground states derived by subtracting the contribution of charging energy from the data in Fig. 1(c) and converting the vertical axis into an energy scale by multiplying the conversion factor $\sim 55 \pm 2$ meV/V defined as the conversion ratio of V_G into energy. The conversion factor was determined from the Coulomb stability diagram in Fig. 1(a). It is found that this QDH has a very large orbital quantization energy difference $\Delta E \sim 10$–20 meV. Moreover, in Fig. 2(d), we can clearly see the lifting of spin degeneracy by Zeeman splitting as well as the diamagnetic Coulomb peak shift and their orbital dependence. The absolute value of the electron g-factor and the diamagnetic coefficients for each orbital state are derived from the data in Fig. 2(d) and summarized in Table I.

From the Zeeman splitting, it is found that this QDH has large electron g-factors in the range $|g| \sim 3$–11; furthermore, the g-factors strongly depend on the orbital states. In the previous study on InAs QDs in the few-electron regime, the decrease in the g-factor for the higher orbital state was reported and was attributed to the weaker coupling between the conduction and valence bands or the extension of the wavefunction into the regions with low In content.[6] In this study, the g-factors show large variation similar to those reported for InAs and InSb nanowire QD devices.[13,14] This orbital-dependent electron g-factor arises from the strong spin–orbit interaction in the InAs QDHs.[13–18] The length of the QDH (~110 nm) is comparable to the spin–orbit length l_{SO} in InAs nanowire QDs ($l_{SO} \sim 125$ nm),[19] whereas it is much shorter than the spin–orbit length in self-assembled InAs QDs ($l_{SO} \sim 410$ nm).[6] This suggests that the spin–orbit scattering events are not significant in this sample, in contrast to those in InAs nanowire QDs.[13] Theoretical calculations

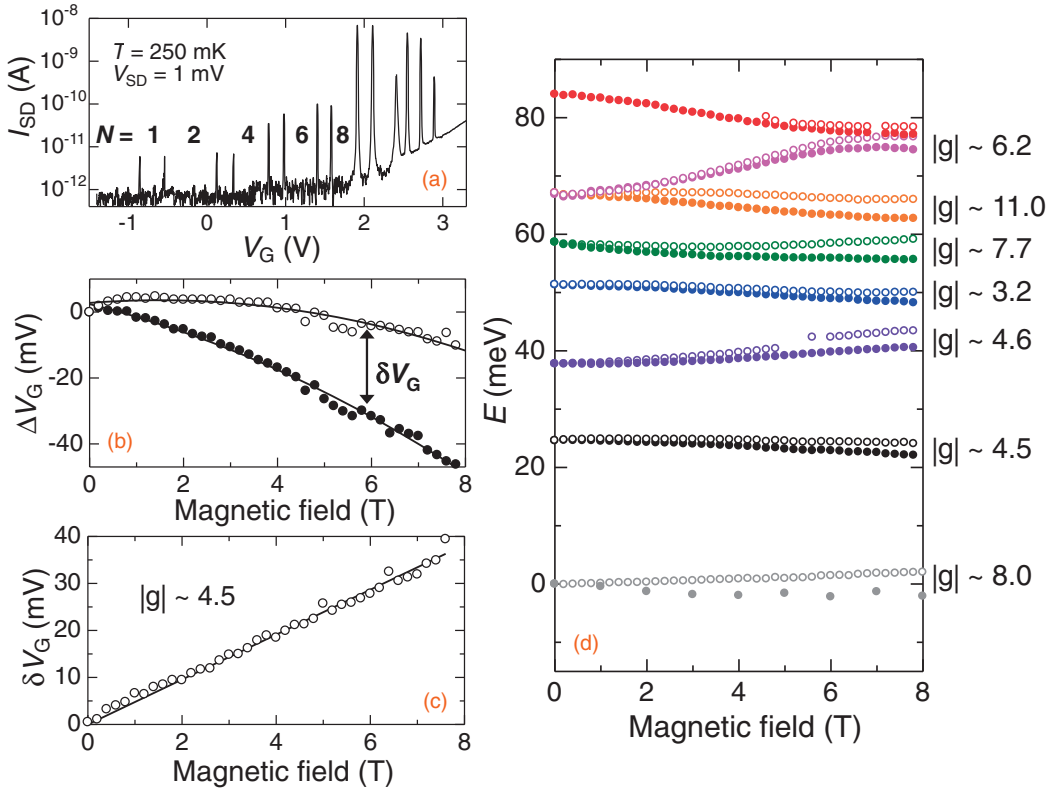

Fig. 2. (a) Linear conductance as a function of gate voltage V_G. (b) Voltage shift of Coulomb peak positions with increasing magnetic field for paired 3rd and 4th Coulomb peaks. The solid lines are fitted to the 3rd and 4th Coulomb peak positions using the same diamagnetic coefficient. (c) Magnetic field evolution of gate voltage spacing δV_G for 3rd and 4th Coulomb peaks. The solid line is a guide for the eye. (d) Magnetic field dependence of ground states derived by subtracting the contribution of charging energy from (c) and converting the vertical axis into an energy scale.

Table I. Electron g-factor, $|g|$, and diamagnetic coefficient (in $\mu eV/T^2$) for each orbital index. The results for the orbital index 1 (1s state) are derived from the magnetic field dependences of the 1st and 2nd Coulomb peak positions. The errors of g-factor mainly come from the error of the conversion factor defined as the conversion ratio of V_G into energy.

Orbital index	$\|g\|$	Diamagnetic coefficient
1	8.0 ± 0.3	12
2	4.5 ± 0.2	−18
3	4.6 ± 0.2	38
4	3.2 ± 0.1	−8
5	7.7 ± 0.3	53
6	11 ± 0.4	−15
7	6.2 ± 0.2	260
8		−170

for metal nanoparticles reported the large variation of the g-factor depending on the spin–orbit scattering time and energy level spacing.[15,16] In our InAs QDHs, the energy level spacing is much larger ($\Delta E \sim 10$–20 meV) than those in metal nanoparticles, and significant contributions from the orbital motion of electrons on the g-factor are expected. Although some theoretical works reported that the g-factor in a semiconductor quantum structure exhibits level-to-level fluctuations,[17,18] the detailed analysis of the g-factor behaviors, which should take into account the orbital contribution and the spin–orbit interaction of InAs QDH, still remains to be carried out.

On the other hand, the diamagnetic shift in the QDs has been widely studied for the excitons in InAs QDs buried in GaAs or InP matrices, and the diamagnetic coefficients on the order of 10–25 $\mu eV/T^2$ have been reported.[20–22] However, there are few experimental reports on the diamagnetic shift in single-electron transistor samples, and this is the first report on the details of the orbital-dependent diamagnetic coefficient in the InAs QD/QDH systems. It is found that the sign of the diamagnetic coefficient changes following the sign change in the orbital angular momentum in the single-electron picture. As the angular momentum and size of the electron wavefunction increases for higher energy states, we find a very strong increase in the diamagnetic shift, e.g., $\gamma_{13-14} \sim 260$ $\mu eV/T^2$ for the 13th and 14th peaks. This very large diamagnetic shift at large electron numbers originates from the large size of the InAs QDHs. Information on the orbital-dependent electron g-factors and diamagnetic shifts in the few-electron regime is useful for understanding the single-electron orbital/spin states and the role of spin–orbit interaction in InAs QDHs,[23] which is important for electrical/magnetic manipulation and readout of single charge/spin states in self-assembled InAs QDHs.[24]

In summary, we have investigated single-electron magneto-tunneling through single self-assembled InAs QDHs coupled to ferromagnetic Ni electrodes. The samples exhibit clear shell structures, reflecting the anisotropic shape of InAs QDHs. The fabricated devices exhibit strongly orbital-dependent large diamagnetic shifts and Zeeman splittings. The observed large diamagnetic shifts reflect the large size of the electron wavefunction in the InAs QDHs. Strongly orbital-dependent large Zeeman splittings imply strong spin–orbit interactions in this system. These properties

strongly suggest that the InAs QDHs are promising for the manipulation of single-electron orbital/spin states by external electric/magnetic fields.

Acknowledgments This work was partly supported by the Japan Science and Technology Agency (JST CREST), Grants-in-Aid from the Japan Society for the Promotion of Science (Nos. 23681029, 25600013, and 25246004), research grants from the Research Foundation for Materials Science and the Casio Science Foundation, Project for Developing Innovation Systems of MEXT, European Community's FP7 through the CRONOS project (grant agreement No. 280879), the Academy of Finland, and the Finnish Cultural Foundation. We also thank CSC Scientific Computing Ltd. for the use of their computational resources.

1) L. P. Kouwenhoven, D. G. Austing, and S. Tarucha, Rep. Prog. Phys. **64**, 701 (2001).
2) J. R. Petta, A. C. Johnson, J. M. Taylor, E. A. Laird, A. Yacoby, M. D. Lukin, C. M. Marcus, M. P. Hanson, and A. C. Gossard, Science **309**, 2180 (2005).
3) F. H. L. Koppens, C. Buizert, K. J. Tielrooij, I. T. Vink, K. C. Nowack, T. Meunier, L. P. Kouwenhoven, and L. M. K. Vandersypen, Nature **442**, 766 (2006).
4) S. Sahoo, T. Kontos, J. Furer, C. Hoffmann, M. Gräber, A. Cottet, and C. Schönenberger, Nat. Phys. **1**, 99 (2005).
5) K. Hamaya, M. Kitabatake, K. Shibata, M. Jung, M. Kawamura, K. Hirakawa, T. Machida, T. Taniyama, S. Ishida, and Y. Arakawa, Appl. Phys. Lett. **91**, 022107 (2007).
6) S. Takahashi, R. S. Deacon, K. Yoshida, A. Oiwa, K. Shibata, K. Hirakawa, Y. Tokura, and S. Tarucha, Phys. Rev. Lett. **104**, 246801 (2010).
7) Y. Kanai, R. S. Deacon, S. Takahashi, A. Oiwa, K. Yoshida, K. Shibata, K. Hirakawa, Y. Tokura, and S. Tarucha, Nat. Nanotechnol. **6**, 511 (2011).
8) R. S. Deacon, Y. Kanai, S. Takahashi, A. Oiwa, K. Yoshida, K. Shibata, K. Hirakawa, Y. Tokura, and S. Tarucha, Phys. Rev. B **84**, 041302(R) (2011).
9) S. P. Guo, H. Ohno, A. Shen, F. Matsukura, and Y. Ohno, Appl. Phys. Lett. **70**, 2738 (1997).
10) K. Shibata, K. Seki, P. J. J. Luukko, E. Räsänen, K. M. Cha, I. Horiuchi, and K. Hirakawa, Appl. Phys. Lett. **99**, 182104 (2011).
11) M. Jung, T. Machida, K. Hirakawa, S. Komiyama, T. Nakaoka, S. Ishida, and Y. Arakawa, Appl. Phys. Lett. **87**, 203109 (2005).
12) The optimization was only done for $N \geq 3$ because the modeling does not work for very low-N. The low-N regime is relatively more sensitive to possible inhomogeneous In concentration profile in InAs QDHs, and thus we find more deviations in that regime, especially for $N = 2$.
13) S. Csonka, L. Hofstetter, F. Freitag, S. Oberholzer, C. Schönenberger, T. S. Jespersen, M. Aagesen, and J. Nygård, Nano Lett. **8**, 3932 (2008).
14) H. A. Nilsson, P. Caroff, C. Thelander, M. Larsson, J. B. Wagner, L.-E. Wernersson, L. Samuelson, and H. Q. Xu, Nano Lett. **9**, 3151 (2009).
15) K. A. Matveev, L. I. Glazman, and A. I. Larkin, Phys. Rev. Lett. **85**, 2789 (2000).
16) P. W. Brouwer, X. Waintal, and B. I. Halperin, Phys. Rev. Lett. **85**, 369 (2000).
17) D. Csontos and U. Zülicke, Phys. Rev. B **76**, 073313 (2007).
18) D. Csontos and U. Zülicke, Appl. Phys. Lett. **92**, 023108 (2008).
19) C. Fasth, A. Fuhrer, L. Samuelson, V. N. Golovach, and D. Loss, Phys. Rev. Lett. **98**, 266801 (2007).
20) T. Nakaoka, T. Saito, J. Tatebayashi, and Y. Arakawa, Phys. Rev. B **70**, 235337 (2004).
21) N. I. Cade, H. Gotoh, H. Kamada, H. Nakano, and H. Okamoto, Phys. Rev. B **73**, 115322 (2006).
22) D. Kim, W. Sheng, P. J. Poole, D. Dalacu, J. Lefebvre, J. Lapointe, M. E. Reimer, G. C. Aers, and R. L. Williams, Phys. Rev. B **79**, 045310 (2009).
23) In contrast with GaAs quantum dots, conventional SDFT calculations used for the modeling above are not sufficient to quantitatively capture the Coulomb oscillation peak positions in this system as a function of B. Extensions of the computational approach including the spin–orbit coupling and ferromagnetic leads are subjects for future work.
24) Application of these QDH samples to tunneling magneto-resistance devices is in progress.